Modelling evapotranspiration using the modified Penman-Monteith equation and MODIS data over the Albany Thicket in South Africa

Gwate, O.; Mantel, Sukhmani K.; Palmer, Anthony R.; Gibson, Lesley

Published in:
Remote Sensing for Agriculture, Ecosystems, and Hydrology XVIII

DOI:
10.1117/12.2245439

Publication date:
2016

Document Version
Author accepted manuscript

Modelling evapotranspiration using the modified Penman-Monteith equation and MODIS data over the Albany Thicket in South Africa

O. Gwate*[a], Sukhmani K. Mantel [a], Anthony R. Palmer[b], Lesley A. Gibson[c]
[a]Institute for Water Research, Rhodes University South Africa, [b]Agricultural Research Council-Animal Production Institute, South Africa, [c]Department of Construction and Surveying, Glasgow Caledonian University, (Scotland, United Kingdom)

ABSTRACT

Evapotranspiration (ET) is one of the least understood components of the water cycle, particularly in data scarce areas. In a context of climate change, evaluating water vapour fluxes of a particular area is crucial to help understand dynamics in water balance. In data scarce areas, ET modelling becomes vital. The study modelled ET using the Penman-Monteith-Leuning (PML) equation forced by Moderate Resolution Imaging Spectroradiometer (MODIS) leaf area index (LAI) and MODIS albedo with ancillary meteorological data from an automatic weather station. The study area is located on the Albany Thicket (AT) biome of South Africa and the dominant plant species is *Portulacaria afra.* The biggest challenge to the implementation of the PML is the parameterisation of surface and stomatal conductance. We tested the use of volumetric soil water content (f_{SWC}), precipitation and equilibrium evaporation ratio (f_{zhang}) and soil drying after precipitation (f_{drying}) approaches to account for the fraction (f) of evaporation from the soil. ET from the model was validated using an eddy covariance system (EC). Post processing of eddy covariance data was implement using EddyPro software. Thef_{drying} method performed better with a root mean square observations standard deviation ratio (RSR) of 0.97. The results suggest that modelling ET over the AT vegetation is delicate owing to strong vegetation phenological control of the ET process. The convergent evolution of the vegetation has resulted in high plant available water than the model can detect. It is vital to quantify plant available water in order to improve ET modelling in thicket vegetation.

Keywords: Penman Monteith equation, eddy covariance, evapotranspiration, Albany Thicket

1. INTRODUCTION

Evapotranspiration represents the combined loss of water from surfaces and through vegetation stomata. ET is one of the least understood processes of the hydrological cycle yet it represents the biggest flux after precipitation [1,2]. Therefore, accurately determining ET is vital, particularly in a context of global changes associated with climate change. It has been established that conventional water resources and methods of water supply are stretched and may not be able to meet global water demand within the purview of these global changes [1,2]. Despite this much effort to increase water availability for agriculture has been through adding blue water and ignoring the need to manage the green water component which could improve water availability for production systems [1,2]. At the same time it is envisaged that in future green water use will increase given that many regions of the world have stretched their blue water resources to the limit and so improving green water management will be critical in improving global production systems [3,4]. This recognition has further increased the impetus to try and understand the ET process on the earth. ET or its energy equivalent, latent heat flux (LE) is crucial in the planetary energy balance which determines global air circulation. Global land-atmosphere modelling initiatives linked to global change studies rely on a better understanding of the exchange of energy, water vapour and carbon dioxide between land- atmosphere systems[5]. However, ET measurement is a daunting task since there are a number of uncertainties associated with accurately characterizing ET [6,7]. Consequently, a number of measurement approaches have been developed including

the Bowen ratio, eddy covariance systems, scintillometers and lysimeters [8,7]. However, these measurement methods are essentially point samples, costly, time consuming, labour intensive and sometimes subject to instrument failure [2]. Therefore, modelling ET remains an important exercise in order to offset the challenges associated with the measurement methods. In addition in a context of patchy measuring stations and general meteorological data scarcity, modelling may be the key to understanding ET. It is against this backdrop that this paper seeks to model ET using a modified Penman-Monteith equation[9].

Much of ET modelling is based on the classical works of Thornthwaite, Priestley and Taylor and Penman-Monteith [10]. It is well established that of these methods, the Penman-Monteith (PM) equation is more theoretically robust [10–13]. The Penman-Monteith formulation is expressed as:

$$\lambda E = \frac{\varepsilon A + \left(\rho C_p\right) D_a G_a}{\varepsilon + 1 + \frac{G_a}{G_s}} \qquad [1]$$

where:

λE - latent heat of evaporation

A - is the available energy absorbed by the surface (net absorbed radiation, R_n minus soil heat flux, G

D_a(kPa) - $e*(T_a) - e_a$is the water vapour pressure deficit of the air (humidity deficit), in which $e*(T_a)$ is the saturation water vapour pressure at air temperature and e_a is the actual water vapour pressure

G_a - Aerodynamic conductance (m s^{-1})

G_s - Surface conductance accounting for evaporation from the soil and transpiration by the vegetation.

γ - psychrometric constant

ρ - Air density (kg m^{-3})

C_p - Specific heat capacity of air (J kg K^{-1})

ε - Slope (s) of the curve relating saturation water vapour pressure to temperature divided by the psychrometric constant (γ) i.e. $\frac{s}{\gamma}$ and is expressed in (kPa K^{-1}).

The classical Penman-Monteith (PM) equation [14] originally evolved as a big leaf model. However, in semi-arid areas characterised by patchy and short vegetation or in areas with LAI < 2.5 [5,1516], such an approach may not be tenable since direct surface evaporation is also critical. Consequently, a number of workers have subsequently enhanced its skill to account for evaporation from many layers [9,16]. This has resulted in the PM equation increasingly becoming a dual or multiple layer model. The dual layer models estimate ET from plants and direct soil ET or ET from two plant types while multi- or three-layer models estimate ET from plants, soil under plants, bare soil or even three types of plants [15].

The partitioning of ET into transpiration and soil evaporation has been a subject of investigation for a while. Evaporation from the soil is essentially a function of volumetric soil water content (SWC) in the upper layers of the soil and it is well known that it follows three stages [17,18]. Stage 1 is designated as an energy limited phase when enough soil water is available for evaporation to occur at a potential rate and is similar to evaporation from a surface of free water (f = 1). This phase ends when the soil moisture content in the upper layer decreases and the soil matric potential reaches a critical value. Stage 2 is symptomatic of a falling ET rate when soil is drying and water availability and soil hydraulic properties that determine the transfer of liquid and vaporized water to the surface limits the soil evaporation rate ($0 < f < 1$). In stage 2, the flux of water

moves in the liquid and vapour forms. On the other hand stage 3 depicts a period when the soil is dry and soil evaporation can be considered negligible ($f = 0$). This stage is essentially a function of soil physical and adsorbing characteristics [17].

However, the biggest challenge in the implementation of the PM equation is the need to characterise canopy and surface conductance or resistances in order to connect potential evapotranspiration (PET) to actual ET [16,18,19]. Leuning et al [16] advanced the application of the PM equation in ET modelling by using ground based routine meteorological data and remotely sensed LAI and albedo. This modelling effort is conveniently termed the Penman-Monteith-Leuning model (PML, [19] and is expressed as:

$$\lambda E = \frac{\varepsilon A_c + (\rho C_{p/\gamma}) D_a G_a}{\varepsilon + 1 + \frac{G_a}{G_c}} + f \frac{\varepsilon A_s}{\varepsilon + 1} \qquad [2]$$

where:

the first part represents evaporation from the canopy and the second that from the soil; the terms A_s and A_c(M J m^{-2}) are energy absorbed by the soil and canopy respectively;

G_c- Canopy conductance (m s^{-1});

f – is a factor which modulates potential evaporation rate at the soil surface expressed by the equilibrium evaporation formulation of [20]; $Eeq,s = \varepsilon A_s/(\varepsilon + 1)$, by $f = 0$ when the soil is dry to $f = 1$ when the soil is completely wet [18]. Eeq,s is equilibrium evaporation from the soil and all other terms have been defined in equation 1.

The PML model built on the preceding modelling work [12,21]. Cleugh et al. [22] found that the PM equation was superior to the aerodynamic resistance–surface energy balance model of calculating ET. They used a simple linear relationship between G_s and the remotely sensed leaf area index (LAI) obtained from the MODIS mounted on the polar orbiting Terra satellite to calibrate G_s . Mu et al.[21] revised the model for G_s by introducing scaling functions that ranged between 0 and 1 to account for the response of stomata to humidity deficit of the air and air temperature. They also introduced a separate term for evaporation from the soil surface. The revised G_s algorithm of [21] resulted in good agreement between predictions of ET by the PM equation and the flux tower measurements. Leuning et al.[16] modified the method of calculating surface conductance (G_s) based on the biophysical understanding of leaf and canopy level plant physiology, radiation absorption by plant canopies and evaporation from the underlying soil surface. Surface conductance (G_s)was seen as a function of G_c, which in turn was influenced by maximum stomatal conductance (g_{sx}) of leaves and energy available at the canopy as well as at the soil surface. In order to parameterize G_s, [16] constrained the fraction of evaporation from the soil as a constant ranging from 0 (no soil moisture) to 1 (saturated soil) but acknowledged that f should be treated as a variable. The g_{sx} and f required to parametrise G_s were estimated using optimization. The new [16] G_s model improved ET estimates when tested against flux tower data in different environments.

Despite, Leuning et al. 's [16] progress in calibrating G_s, the determination of the f value as a variable rather than a constant remained a challenge in order to account for evaporation from the soil particularly in patchy and short canopies. Pursuant to this, [19] used the ratio between precipitation and equilibrium evaporation rate as an indicator of soil water availability to obtain f values, conveniently called f_{zhang} over successive 8 days intervals. However, for arid zones characterized by irregular precipitation which causes rapid increases in soil moisture during rain followed by extended drying periods, [18] postulated that (f_{zhang}) was inadequate for semi-arid regions. They tested three different approaches to estimate the temporal variation of f:

(i) using direct soil water content measurements;
(ii) application of the f_{zhang} method of [19]; and
(iii) Application of the (f_{drying} approach.

Morillas et al. [9] found that determining the (f) component as a function of soil drying after precipitation (f_{drying}) yielded better results than determining the f component as either a function of precipitation and equilibrium evaporation ratio (f_{Zhang}) or determining it as a function of soil water content (f_{SWC}). The full description of the PML model is found in [18].

This work tests the performance of the PML equation[16],[18] over the AT of South Africa. The study area presents interesting space for testing the model since it is located in a dry landscape dominated by succulent vegetation. It has been established that such vegetation type has high water storage capacity within its tissues and has a very high water use efficiency [23–25]. These characteristics predispose the land-atmosphere water vapour transfer to be strongly coupled to plant phenological dynamics. Therefore, it will be interesting to test if routine meteorological data from automatic weather station (AWS) and remotely sensed LAI and albedo could capture the dynamics of evaporation over such a complex landscape.

1. Material and methods

2.1 Experimental site

The study area lie on the eZulu Private Game Reserve situated about 70km west of Grahamstown, South Africa (33° 01' 08.929" S 26° 04' 47.860" E) on the AT biome. The AT has been recognised as a biodiversity hotspot characterised by succulents, deciduous and semi-deciduous woody shrubs and dwarf shrubs, geophytes, annuals and grasses. The understorey comprises of a relatively high diversity of dwarf succulent shrubs and forbs, mainly *Crassulaceae* and *Aizoaceae* [26]. The dominating vegetation type on the field site was *Portulacaria afra*, a plant known for its Crassulacean Acid Metabolism (CAM) photosynthesis. Consequently, there is renewed interest for the plant in South Africa as it is widely used in land rehabilitation as a pioneer species[27]. Modelled annual pan evaporation is about 1963.9 mm while long-term mean annual rainfall is around 493.7 mm[28]. The area has a bimodal rainfall pattern, with mean long-term monthly maxima around October-November and in March. Further details of the study area can be found in the accompanying paper [29].

2.2 Data

2.2.1 Micrometeorological data

Calibration and validation data was collected using an Integrated CO2/H2O Open-Path Gas Analyser and 3D Sonic Anemometer (IRGASON, Campbell Scientific Inc., Logan, Utah, USA). It is an in-situ, open-path, mid-infrared absorption gas analyser integrated with a three-dimensional sonic anemometer. The gas analyser provides measurements of absolute densities of carbon dioxide and water vapour, while the sonic anemometer measures orthogonal wind components. The IRGASON was located over horizontally uniform vegetation at 2.65 m above the ground. A shielded (R.M. Young 41303-5A 6-Plate Solar Radiation Shield) temperature and relative humidity probe (HC2S3, Campbell Scientific Inc., Logan, Utah, USA) was installed so that it measures temperature at the same height as the sample volume of the IRGASON in order to measure air that had similar characteristics. Both the IRGASON and the temperature probe were connected to the EC100. Further, a fast response fine wire thermocouple (FW05: 0.0005 in /0.0127 mm, Campbell Scientific Inc., Logan, Utah, USA) was placed between the upper and lower arms of the IRGASON. Other bio-meteorological sensors installed included soil heat flux (G), (SWC), air and soil temperature probes. The soil heat flux (G) was measured using four soil heat flux plates (HFP01, Campbell Scientific Inc., Logan, Utah, USA). The plates were placed at a depth of 80 mm below the soil surface. A system of parallel soil thermocouple probes (TCAV) were installed at depths of 20 and 60 mm to measure soil temperature. A soil thermocouple probe measures temperature at four locations, or junctions, each consisting of a type E thermocouple wire (chromel-constantan) that is enclosed within a stainless steel tube [30]. The thermocouple works in conjunction with the soil heat flux plate to calculate the heat flux at the surface of the soil. Volumetric soil water content (CS616, Campbell Scientific Inc., Logan, Utah, USA) was measured in the upper 60 mm of the soil. The installation of the heat flux plates, the soil temperature thermocouples and the water content reflectometer was done following instructions provided by [30]. The net radiation was measured using a net radiometer (NR-lite2, Kipp & Zonen, Netherlands). Table 1 presents the details of the instrumentation at the site.

Table 1. Summary of instruments at the eZulu EC station

Biometeorplogical variable	Instrument
Net radiation (W m^{-2})	Two net radiometers (NR-lite2) (Kipp & Zonen, Netherlands)
Air temperature (°C) and Relative humidity (RH, %)	HC2S3 Temperature and relative humidity Probe (Campbell Scientific Inc., Logan, Utah, USA)
Soil heat flux (W m^{-2})	4x soil heat plate (HFP01 , Campbell Scientific Inc., Logan, Utah, USA)
Soil temperature (°C)	2x Averaging soil thermocouples probe (TCAV, Campbell Scientific Inc., Logan, Utah, USA)
Air temperature (°C)	Fine wire thermocouples (FW05: 0.0005 in /0.0127 mm , Campbell Scientific Inc., Logan, Utah, USA)
Volumetric water content (ratio)	Water content reflectometer (CS616, Campbell Scientific Inc., Logan, Utah, USA)
Wind speed (m s^{-1}) and direction (degrees)	IRGASON

Bio-meteorological probes were connected to a CR3000 data logger (Campbell Scientific Inc., Logan, Utah, USA) for data recording. Data was saved onto a 2 GB compact flash memory card with the capacity to store up to six weeks of high frequency (10 Hz) data. The EC system was powered by two solar panels (SDT800 - 12V 80W Solar Module that charge four 100 AmpHour deep cycle batteries (Deltec - SMF 1250 High Cycle).

2.2.2 Scientific grade automatic weather station data

In order to force the PML, meteorological parameters required include solar radiation, air temperature, relative humidity (RH), wind speed and rainfall (Table 2). Daily meteorological data was obtained from the scientific grade automated weather station (AWS) in situ. These data are completely independent from the EC system and provides an opportunity to compare ET derived from a routine weather station and that from the EC system.

Table 2. Summary of instruments at the automated weather station

Weather parameter	Instrument
Solar radiation (MJ m^{-2})	Pyranometer (LI-200SA*)
RH (%) and Air temperature(°C)	Vaisala HMP60 Temp/Humidity probe (HMP60)
Wind speed (m s^{-1}) and direction (degrees)	R.M. Young wind sentry wind set (10FT LEAD, Model 03001)
Rainfall	Te525mm-l texas electronics rain gage 0.1MM (0.00394 INCH, TE525mm-L)

2.2.3 MODIS data

The Moderate Resolution Imaging Spectroradiometer (MODIS) is an instrument on Terra and Aqua satellites that provide comprehensive series of global observations of the Earth's land, oceans, and atmosphere in the visible and infrared regions of the spectrum. The study used the MODIS LAI that uses the MOD15A2 fPAR/ LAI algorithm [31] to force the PML model. This is a freely available product with an 8-day temporal and 1km spatial resolution. We obtained MOD15A collection 5 from the ORNL-DAAC (http:/daaac.ornl.gov) to get average LAI values to force the PML. The fPAR and LAI are biophysical variables that describe canopy structure and are related to functional process rates of energy and mass exchange [31]. It should be observed that LAI is a state parameter in the PML and PMP models that facilitates the partitioning of fluxes in the land- atmosphere continuum. Remotely sensed albedo required for the calculation of net radiation was obtained also from the MODIS program. We applied the nadir bidirectional reflectance distribution function adjusted reflectance (NBRDF) product (MCB43B4, https://lpdaac.usgs.gov/) with a 1km spatial and 8 day temporal resolution. Subsequently, the equation developed by [32] was applied using the six MODIS bands in order to derive shortwave albedo (and scaled with 0.0001) as follows:

$$\propto_{short} = 0.160 \propto_1 + 0.291 \propto_2 + 0.243 \propto_3 + 0.116 \propto_4 + 0.112 \propto_5 + 0.081 \propto_7 - 0.0015 \quad [3]$$

where:

$\propto_{short}$ is shortwave albedo and $\propto_1$ is the spectral band

2.3 Data analysis

2.3.1 Micrometeorological data

Micrometeorological data was downloaded from the eddy covariance system and sorted for further analysis in EddyPro 6.0 (https://www.licor.com/env/products/eddy_covariance/eddypro.html) software. All raw 10 Hz data were firstly processed into half-hourly averages using LoggerNet (4.3) software (Campbell Scientific Inc., Logan, Utah, USA). Post processing included axis rotation for tilt correction was implemented using double rotation and the linear detrending method was applied to remove turbulent fluctuations. Time lag compensation was implemented using covariance maximization with default. Statistical tests for raw data screening, such as spike removal, amplitude resolution, drops outs, absolute limits, discontinuities, time lags, skewness and kurtoisis, steadiness of horizontal wind, angle of attack, were implemented following [33]. Random uncertainty estimation was implemented following [34]. The method described by [35] was used to filter out data that failed steady state statistical tests. This method uses the values (0, 1 and 2) as an overall quality flag with fluxes flagged 2 not used in ET computation. Rejected and missing data were filled using the method of mean diurnal variations (MDV [36]The EC footprint was estimated using the method of [37]. The Webb-Pearman-Leunning (WPL) correction was not implemented since the IRGASON internally corrects for density fluctuations.

2.3.2 Determining proportion of soil evaporation

We tested three methods for determining the fraction of soil evaporation (f) in order to fully implement the PML equation. We applied the f_{zhang} [19], f_{drying} [18] and used measured volumetric soil water content (f_{SWC}) to parameterise surface conductance. The f_{zhang} method is based on determining the proportion of evaporation from the soil as a function of accumulated daily precipitation and equilibrium ET (Eeq, s, i) both in mm over N days expressed as:

$$f_{Zhang} = \min\left(\frac{\sum_{i=15}^{i} P_i}{\sum_{i=15}^{i} Eeq,s,i}\ ,\ 1\right) \qquad [4]$$

where P_i is the accumulated daily precipitation and Eeq, s, i is the daily soil equilibrium evaporation rate for day i.

On the other hand the f_{drying} estimates daily values of f in two ways. Firstly, it adapts the f_{Zhang} method to days that received effective rainfall and secondly, if no effective precipitation was received, f is obtained as a function of soil drying after effective precipitation. The f_{drying} method is expressed as:

$$f_{Zdrying} = \left(\min\left(\frac{\sum_{i=15}^{i} P_i}{\sum_{i=15}^{i} Eeq,s,i}, 1\right) \text{ when } P_i > \mathrm{P_{min}} \qquad [5]$$

$$= \quad f_{LP} \exp(-\acute{\alpha}\Delta t) \text{ when } \ P_i < \mathrm{P_{min}}$$

where P_i is accumulated effective precipitation for the last i days, $\mathrm{P_{min}}$ is effective precipitation, f_{LP} is the f value for the last effective precipitation day, Δt is number of days between this and the current day i and $\acute{\alpha}$ ($\mathrm{day^{-1}}$) is a parameter controlling the rate of soil drying, higher $\acute{\alpha}$ values reflecting higher soil drying speed. Morillas et al.[18] considered $\acute{\alpha}$ as a constant and estimated it by optimmization, although they acknowledged $\acute{\alpha}$ is related to air temperature, wind speed, vapor pressure deficit, and soil hydraulic properties and hence, it should be treated as a variable. Based on the CLIMWAT database [38], daily effective precipitation was estimated at 1.48 mm for our study site.

3.2.3 Calibration and validation

We applied the three methods of determining the rate of drying in order to calibrate surface conductance specific to the study site. However, values for $\acute{\alpha}$ and maximum stoamatal conductance (g_{sx}) were obtained through optimization in the R-3.1.1 software environment using rgenoud[39,40]. The calibration period spanned 100 days (DoY 294, 2015)- DoY 28, 2016). Calibration sought to find locally specific values of g_{sx} and $\acute{\alpha}$. The optimization sought to find the values of g_{sx} and α' that minimised the difference between the predicted and observed ET over a given number of days (N):

$$F = \frac{\sum_{i=1}^{N} |E_{est,i} - E_{obs,i}|}{N} \qquad [6]$$

where:

$E_{est,i}$ is estimated ET, $E_{obs,i}$ is observed ET during the same day and N is the total sample number and F is the function to be minimized.

Model validation took place between DoY 51 to DoY 201 (2016). The standard major axis (SMA) model II regression was used to determine the relationship between the observed and predicted ET. The SMA was found suitable for ET data since it can handle errors and uncertainties in x and y axis variables [41] Model performance was evaluated using the root mean square (RMSE), RMSE-observations standard deviation ratio (RSR) and Mean absolute error (MAE) as well as percent bias. Willmott [42] noted that no single model evaluation index can adequately describe model performance and as such it is prudent to use different indices simultaneously. The mean square error (MSE) was partitioned into systematic and unsystematic and mean square error (MSE) in order to establish sources of error in the RMSE [43]. Systematic MSE is given by:

$$MSE_s = N^{-1} \sum_{i=1}^{n} \ \hat{P}_i - O_i)^2 \qquad [7]$$

where:

MSE_s is systematic MSE, O_i is observed ET and $\hat{P}_i$ is derived from $\hat{P}_i = a + bO_i$, i.e the linear regression between the observed and modelled ET. The unsystematic MSE is expressed as:

$MSE_u = N^{-1} \sum_{i=1}^{n} (P_i - \hat{P}_i)^2$ [8]

The MAE was used since it is less sensitive to extreme values than RMSE and it avoids the physically artificial exponentiation that is an artefact of statistical mathematical reasoning from which RMSE comes from. The RSR is also a valuable index since it helps to give insights as to a measure of what is considered a lower RMSE [44]. Further to these the coefficient of determination (R^2) and the slope and y-intercepts were investigated. Percent bias (PBIAS) was also considered in order to determine model under- or over-estimation bias. Sensitivity of the model to remotely sensed inputs (leaf area index, LAI and albedo) and aerodynamic components was assessed to determine the influence of variations in these input parameters on total ET.

2. RESULTS

3.1 Environmental conditions during the calibration period

Mean daily environmental conditions during the calibration period are shown in table 1. The coefficients of variation for wind speed, soil water content, soil and air temperature were lower compared to other environmental variables (Table 1).

Table 1. Environmental conditions during calibration period

Environmental parameter	Mean± SD	Coefficient of variation
Air temperature	22±4	18
Soil temperature	30±4.8	16
Wind speed	1.7±0.6	16.5
VPD	1378.2±620.6	45
RH	63±10	15.9
Soil water content	0.084±0.02	19.6
LAI	0.49±0.11	22
ET	1.55±1.34	86.5
Rainfall	0.91±3.1	344.8
Solar radiation	277.3±82	30

A total of 92.2 mm of rainfall was received during the calibration period and a prolonged dry spell prevailed between DoY 347 (2015) and DoY 6 (2016). Daily maximum rainfall of 19.4 mm was recorded and rainfall was the most variable environmental parameter as shown by the high coefficient of variation (338.8%). Soil water content ranged from 0.063 to 0.126 mm mm^{-3} and it was strongly coupled with rainfall (Fig 1a and b).The ET pattern generally followed that of rainfall and SWC (Fig. 1a and b) although total ET exceeded rainfall received by about 35%. However, significant ET of up to 2.36 mm day^{-1} occurred during a dry spell between DoY 346 (2015) to DoY 6 (2016) when soil water content was at the lower end between 0.063 and 0.07mm mm^{-3} (Fig. 1 a and b). Soil temperature was consistently higher than air temperature throughout the calibration period (Table 1 and Fig 1c). Average daily wind speed, RH, solar radiation and VPD were

generally high enough (0.8 -3.65 m s^{-1}, 39.8- 85.65%, 61 - 385 W m^{-2} and 380-3334.9 (Pa) respectively to aid the ET process (Fig 1d-g). Figure 1h presents trends in the LAI and 8 day accumulated ET to match the availability of MOD15 LAI. The LAI ranged from 0.3 to 0.7 and it should be noted that minimum accumulated ET occurred between DoY 353 and 361 when the LAI was at 0.4.

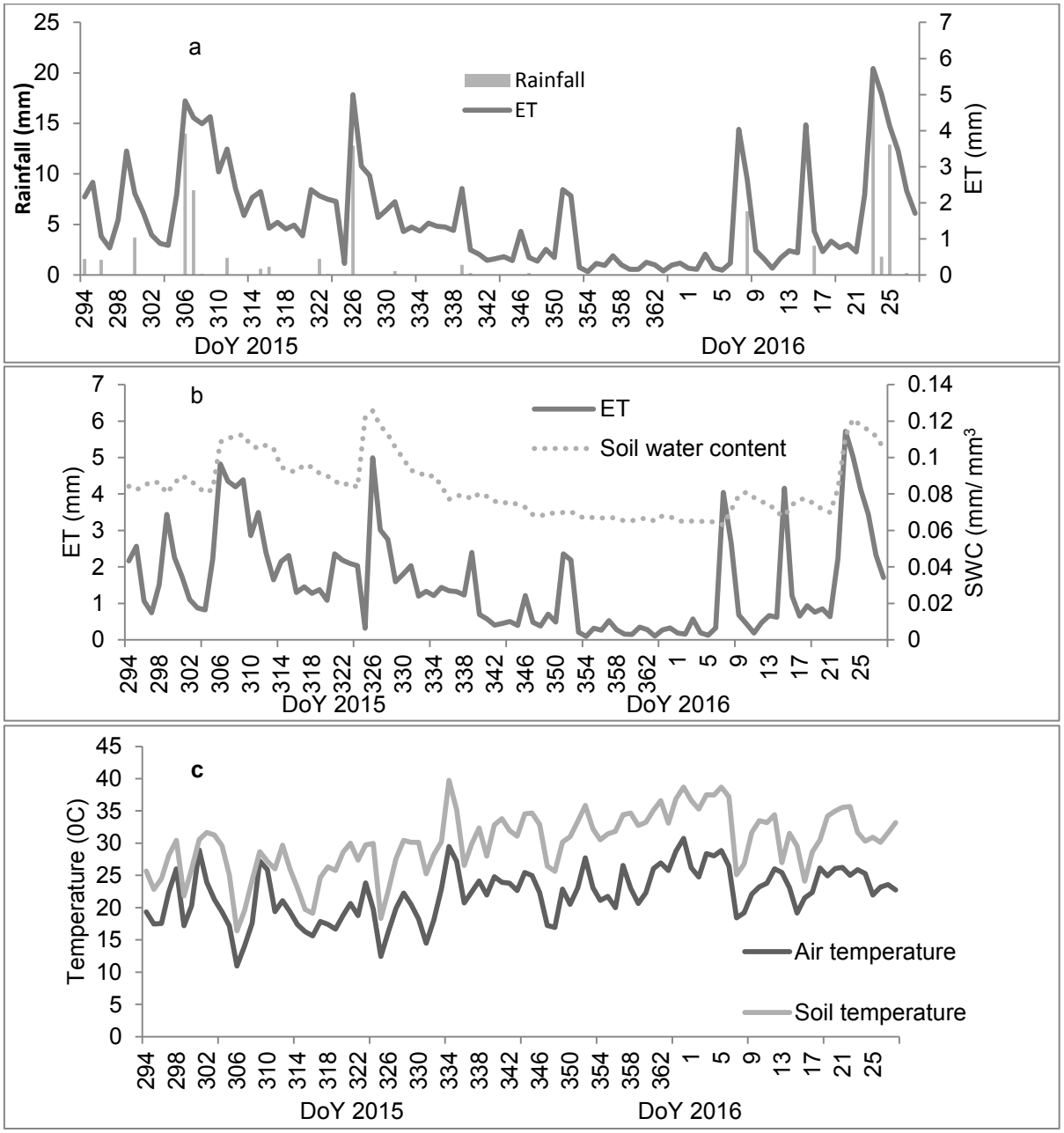

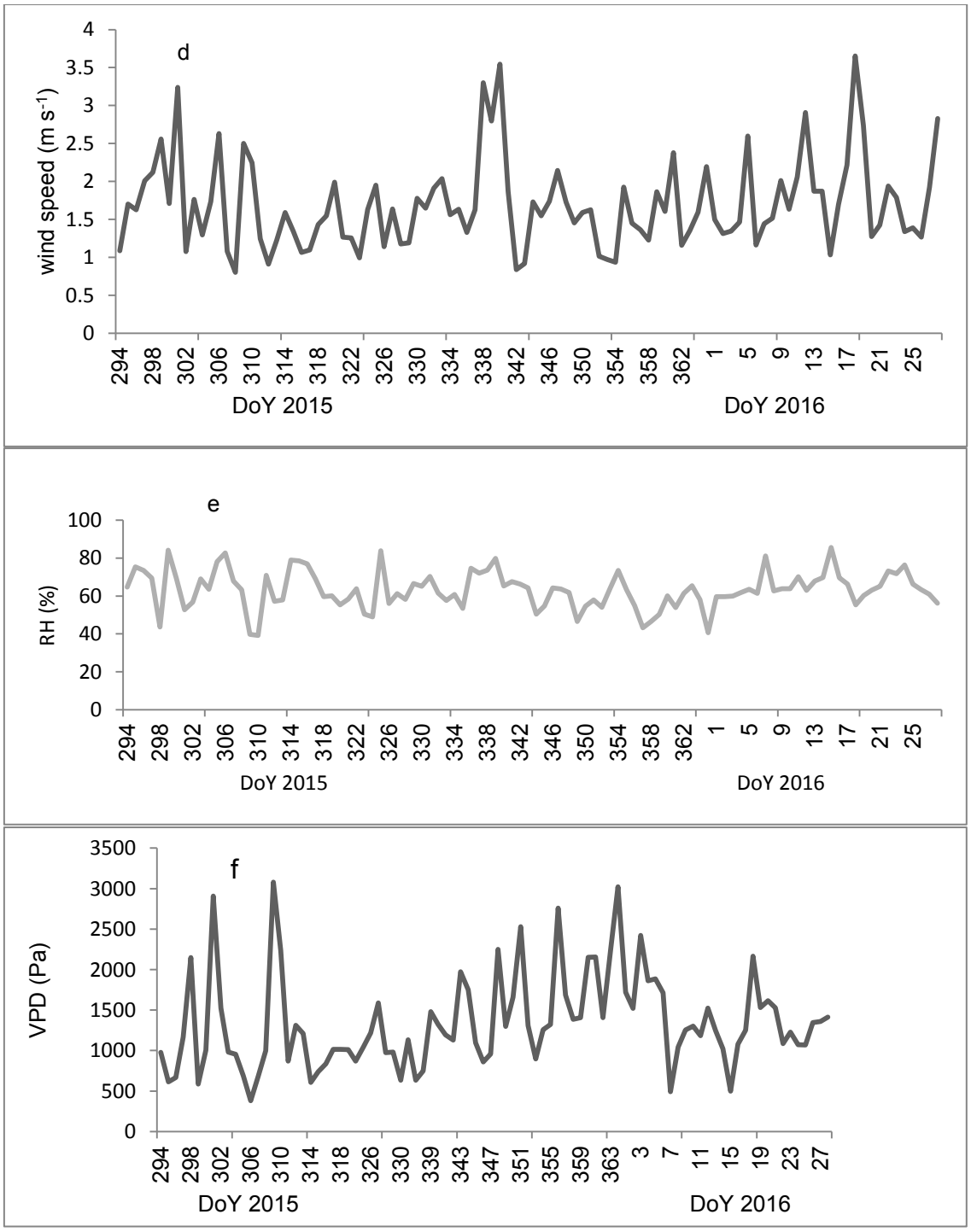
d
wind speed (m s-1)
4
3.5
3
2.5
2
1.5
1
0.5
0
294 298 302 306 310 314 318 322 326 330 334 338 342 346 350 354 358 362 1 5 9 13 17 21 25
DoY 2015
DoY 2016
e
RH (%)
100
80
60
40
20
0
294 298 302 306 310 314 318 322 326 330 334 338 342 346 350 354 358 362 1 5 9 13 17 21 25
DoY 2015
DoY 2016
f
VPD (Pa)
3500
3000
2500
2000
1500
1000
500
0
294 298 302 306 310 314 318 326 330 339 343 347 351 355 359 363 3 7 11 15 19 23 27
DoY 2015
DoY 2016

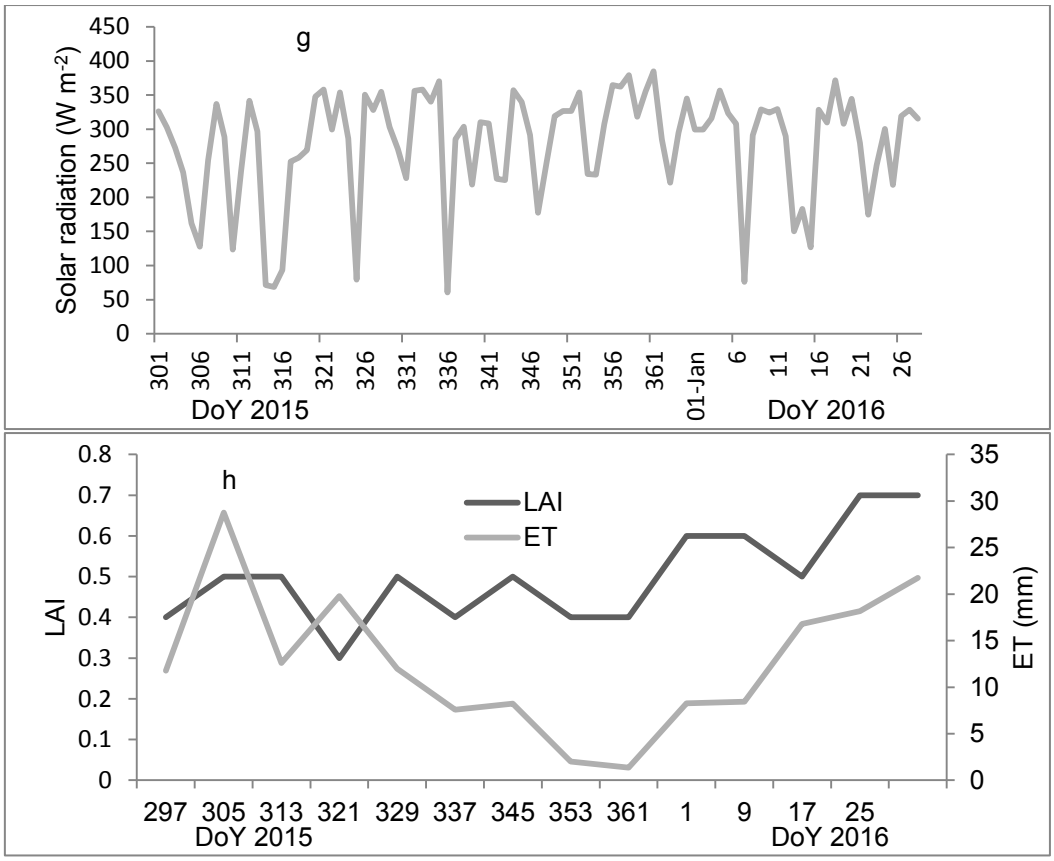

Figure 1. Trends in environmental condition during the calibration period: a) rainfall and evapotranspiration (ET), b) Soil water content and ET, c)air and soil temperature, d) Relative humidity (RH), e) Wind speed, f) Vapour pressure deficit (VPD), g) solar radiation and h) leaf area index (LAI) and ET.

3.2 Model calibration

Table 2 presents the calibration results for optimised values for g_{sx} and α for the AT site. Using the f_{Zhang} approach and the soil volumetric water content to calibrate conductance, the model yielded higher stomatal conductance compared to that when f_{drying} was used (Table 2). When the measured SWC and f_{Zhang} approaches were implemented to account for soil evaporation, g_{sx}, values were similar (Table 2).

Table 2. Optimized values of maximum stomatal conductance (g_{sx}) and the rate of soil drying (α').

Model	**Maximum stomatal conductance (g_{sx})**	**Rate of soil drying (α')**
f_{drying}	0.009	0.32
f_{Zhang}	0.0108	N/A
f_{SWC}	0.0109	N/A

3.3 Model Validation

The model performed better using the f_{drying} approach with a MAE of 1.24 mm d^{-1} and RSR of 0.97 and unsystematic mean square error of 80% (Table 3). This was followed by the f_{Zhang} approach which had a MAE of 1.1 mm d^{-1} and an RSR of 1.04. With respect to the f_{SWC} approach, the MAE was 0.86 mm d^{-1} and an RSR of 1.13. Although the SWC approach yielded inferior results than that of the other two approaches, its MAE was the lowest. All the three approaches for estimating soil evaporation underestimated ET as shown by positive PBIAS values (Table 3). The f_{drying} formulation model predicted ET within 14% of the observed. Figure 2 shows the slope intercept and the R^2 of the relationship between the observed and modelled ET.

Table 3. Evaluation of the PML model

Model	**MAE**	**RMSE**	**RSR**	**PBIAS**	**Systematic MSE**	**Unsystematic MSE**
f_{drying}	1.24	1.41	0.97	35	20	80
f_{Zhang}	1.1	1.48	1.04	36	51	49
f_{SWC}	0.86	1.52	1.13	50	30	26

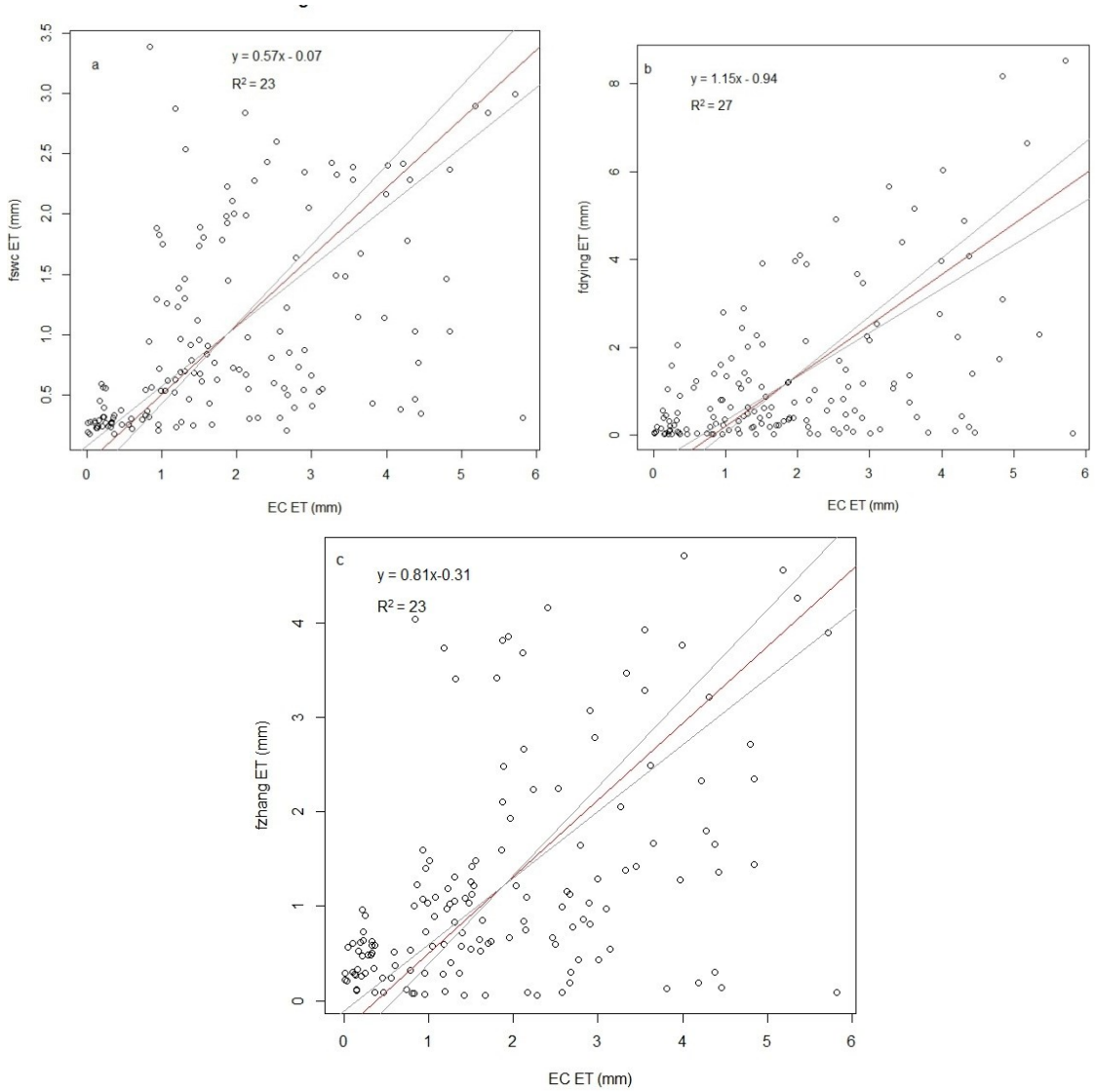

Figure 2. Relationship between the observed Eddy covariance system evapotranspiration (EC ET) and modelled ET: a) f_{SWC}, b) f_{drying} and c) f_{Zhang} approaches for accounting soil evaporation.

3.4 Trends in measured and modelled evapotranspiration (ET)

Between DoY 51 and 145, the pattern of modelled ET followed that measured by the EC while between DoY 146 and 162 the modelled could not reproduce the observed pattern of ET as the modelled were consistently low (Fig. 2). However, from DoY 163 to 201, the trends in ET were similar. Figure 2b also shows that there were some spikes when using the f_{drying} approach which resulted in the over estimation of ET during some days. The f_{SWC} approach resulted in consistently lower ET throughout the validation period compared to the other two approaches (Fig 2). Between DoY 51 and 100, the f_{Zhang} approach captured the dynamics in ET better than the other approaches (Fig 2c).

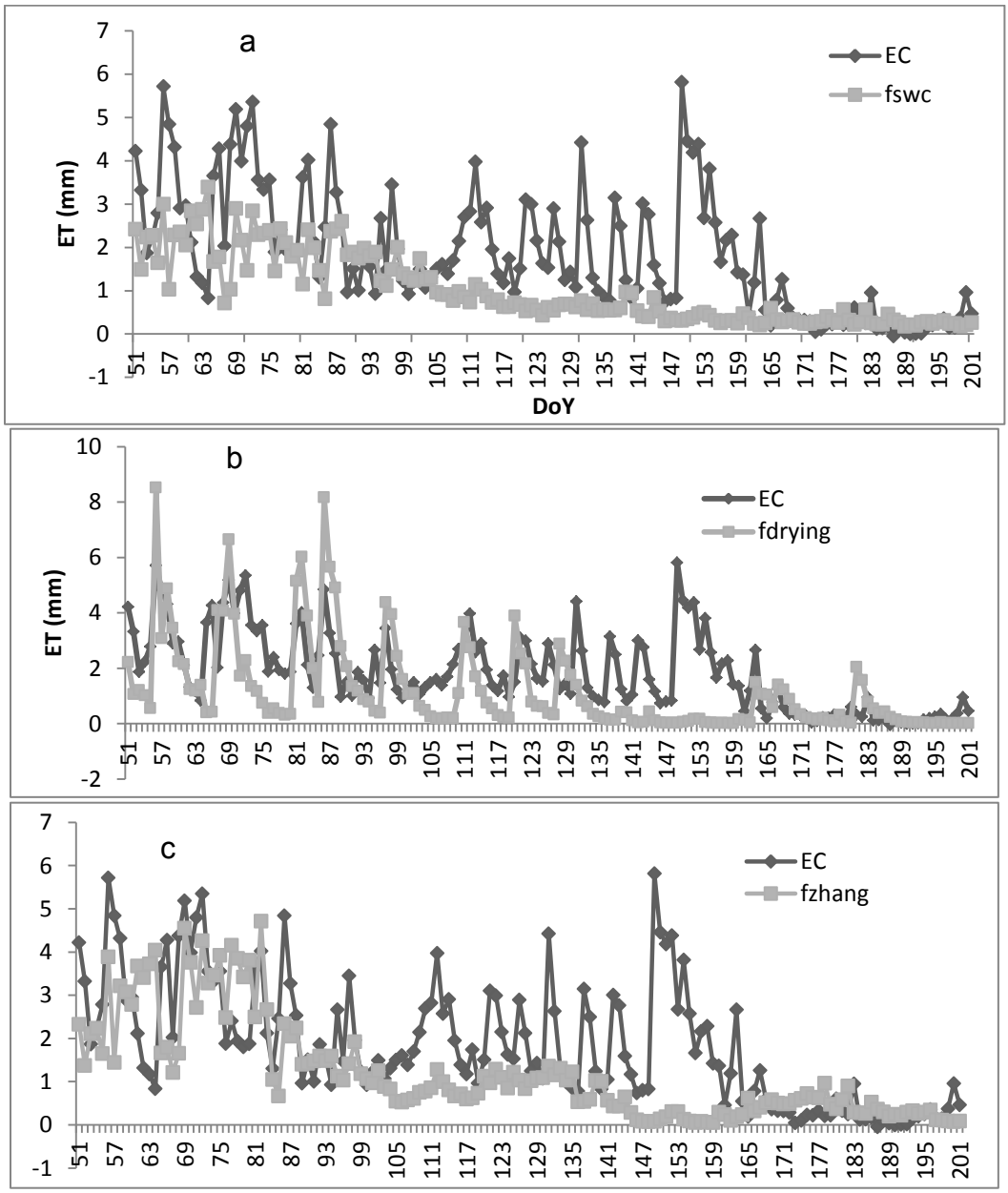

Figure 3. Trends in observed eddy covariance system (EC) evapotranspiration (ET) and modelled evapotranspiration at eZulu station: a) f_{SWC}, b) f_{drying} and c) f_{Zhang} approaches for accounting soil evaporation.

3.5 Model sensitivity

Model sensitivity analysis revealed that it was critical to accurately define the components of G_a in order to successfully use the PML. Table 1 suggests that the model can easily overestimate ET if the canopy height, the height of wind speed measurement and the wind speed at canopy are not properly defined. By increasing the height of wind speed measurement, surface resistance to evaporation decreases leading to an increase in ET (Table 4).

Table 4. Model sensitivity to Wind speed and wind speed measurement height

Canopy height (m)	**Height of wind speed measurement (m)**	**Total ET (mm)**
0.12	2	1158.7
0.5	2	1025.6
0.5*	2	572.3
0.5**	0.5	451.7

*wind speed at 2m was extrapolated to wind speed at 0.5m (canopy height) using the power law and height of wind measurement was maintained at 2m.

**wind speed at 2m was extrapolated to wind speed at 0.5m (using the power law) and canopy height (0.5m)

Furthermore, sensitivity analysis has also shown the importance of LAI in partitioning ET between ET_s and ET_c. The analysis shows that at low LAI values soil evaporation (ET_s) is higher than transpiration (ET_c, Table 5).

Table 5. Model sensitivity to the leaf area index (LAI)

LAI	$\boldsymbol{ET_s}$	$\boldsymbol{ET_c}$	**Total ET**	**Percentage** $\boldsymbol{ET_s}$
1	446.1	124.5	570	78
2	277.6	318.1	595.7	47
2.5	214	403.8	618	35
3	162.21	476.91	639.12	25
3.5	121.82	537.2	659.12	19

Albedo is also another important input into the PML model and as such it has to be accurately defined. For example, analysis revealed that doubling albedo from 0.08 to 0.16 results in a decrease of about 10% in total ET whilst a 15% increase in albedo from 0.35 to 0.40 results in a 10.3 decrease in ET. At the same time an increase of 15% of albedo from 0.3 to 0.35 results in a decrease of 9.2% in ET (Table 6).

Table 6. Sensitivity of PML to albedo

Albedo	ET
0.08	597.5
0.16	537.7
0.2	507.8
0.23	485.3
0.27	455
0.3	431.7
0.35	392.7
0.40	352

3. DISCUSSION

4.1 Environmental conditions

The calibration took place under varied conditions ranging from great moisture deficit (SWC < 0.065) to higher moisture content of over 0.12. Solar radiation and wind speed also varied greatly. Therefore results derived from model testing can be considered to be truly representative of environmental dynamics in the study area. Ideally, it could have been interesting to optimise model parameters for both growing and non-growing season separately. However, [18] could not detect any improvements in model fit by calibrating the model for specific time periods like during the growing and non-growing season. Hence our calibration time period is unlikely to have influenced the results. Although some environmental parameters were variable during the calibration period, the average conditions presented in Table 1were conducive for ET to take place. Results also suggest that the study site was essentially water limited as shown by relatively high atmospheric demand with mean VPD of 1378.2 Pa (Table 1). In addition ET trends essentially followed those of rainfall and SWC. It is widely accepted that ET is primarily driven by SWC. However, it is interesting to note that during periods of low SWC, significant ET of up to 2.36 mm d^{-1} still occurred. This suggests that the observed ET may not be necessarily related to SWC measured by soil moisture sensors buried at 25 mm below the surface. It is well established that the convergent evolution of thicket vegetation similar to the study site has resulted in high water storage in plant tissues to allow plant function during extended periods of moisture deficit [23,25]. In addition, during the calibration period ET was about 35% greater than rainfall received. We therefore, speculate that the high water storage capacity associated with succulent vegetation could be the main driver of ET during periods of soil moisture deficits. In addition there is a distinct possibility that some of these plants could be taping ground water to sustain high ET during periods of SWC deficit. In vegetated surface, the LAI is often one of the key biotic determinants of ET. We had anticipated that maximum LAI would coincide with maximum accumulated ET in Figure 1h. However, the LAI and ET trends were not in unity with ET trends. This lack of consistency is suggestive of strong vegetation phonological controls to the ET process. This was not surprising since it is well established that thicket vegetation has evolved to control stomata opening to optimise water use during day light and tend to have low stomata density [24,44]. In addition, it is widely accepted that in areas where the LAI is < 2.5, surface and under-canopy ET becomes more prominent than canopy transpiration [5,18,46]. Sensitivity analysis results also showed that soil ET was important in areas of low LAI.

Therefore, modelling ET in complex vegetation such as the AT should proceed with a thorough understanding of a variety of factors controlling ET and this makes the modelling process a daunting task.

4.2 Model performance

Table 2 presents results of optimization to calibrate canopy and surface conductance. These results suggest that stomatal conductance is relatively high in the AT. There is a general belief that such thicket vegetation tends to close stomata during daylight hours to optimise water use [24,25]. As such, one would have envisaged relatively low stomatal conductance in such vegetation which lead to low ET. However, in the accompanying paper [29] we observed that ET took place during both day light and night hours. Therefore, despite strong phenological control to water use, the optimised g_{sx} are realistic and indicate the dynamics of vegetation behaviour in the study site. In addition, the optimised values are within the published ranges of g_{sx} (for example [47,16,17]. At the same time, the lower g_{sx} using the f_{drying} approach resulted in systematic underestimation of ET while the under estimation of ET using the SWC and f_{Zhang} approaches could be a result of the under estimation of plant water available for ET by the SWC sensors. As already pointed out, the high water storage potential and the possibility of vegetation accessing ground water, provide extra plant available water to drive ET in such landscapes. Ideally, temporal dynamics in g_{sx} and α' are required to accurately reproduce the daily pattern of ET. However, the use of these optimised constants showed that reasonable results can still be achieved. Therefore, future work needs to develop models that will capture temporal dynamics in these variables instead of using constants.

The observed trends in modelled ET are symptomatic to limitations of the model in areas characterised by strong biotic control of the ET process. The sporadic spikes in ET from f_{drying} approach were linked to rainfall events, suggesting that the model considered maximum soil ET since the soil will be saturated. However, owing to biophysical controls to ET, highest soil ET may not be observed even when soil moisture is not limiting. All the three approaches were better able to capture the pattern of measured ET when SWC was high. During periods of great SWC deficits, the approaches underestimated ET. This failure by the approaches is linked to plant available water. We speculate that although SWC was low, plant available water was high owing to the convergent evolution of the AT vegetation related to great water storage capacity. In addition, there is a distinct possibility that some of the plants were tapping ground water. Therefore, the observed ET may not be related to SWC at the upper layers of the soil.

We also analysed the performance of different approaches of parameterising surface and canopy conductance. We adopted thef_{drying}, f_{Zhang} and the use of SWC combined with optimization to parametrise conductance. Although the SWC approach yielded the lowest MAE, the model performed less well when compared to the other two approaches. This underlies the importance of using more than one model evaluation criteria [43, 44]. Our results are consistent with the views held by Willmott [43] that correlation measures such as R^2 maybe be misleading in model evaluation and they should be interpreted with caution. The results provide evidence that R^2 does not necessarily indicate the robustness of the model results asf_{Zhang} and f_{SWC} had similar R^2 yet the former performed better than the latter. Overall, the poor coefficients of determination can partly be explained by the complexities of the land- atmosphere transfer over the thicket vegetation. Owing to the convergent evolution of succulent vegetation to store and optimise water use, the ET process does not respond linearly to available plant water that drives ET in these dry environments. In an accompanying paper [29], we obtained low R^2 between measured ET against biotic and abiotic controls to ET using both linear and non-linear regression in the study site. Hence the coefficients of determination were weak owing to complex vegetation phenological controls to ET. All the three conductance modelling approaches yielded higher values of both MAE and RMSE compared to those obtained by [18] in Mediterranean drylands of Spain characterised of *Hormatophiylla spinose*, *Festuca scariosa*, *Genista pumila* and *Hormatophiylla spinose* species. The differences can be explained by the varying vegetation characteristics. ThHowever, suffice to note that using the similar formulation [19] found RSME of 1.56 mm d^{-1} and 1.13 mm d^{-1} at Dargo High Plains and Howard Spring in Australia respectively. These results were similar to those presented in Table 3 of this paper. However, the R^2 found by [9] ranged from 0.24-0.59.We found better model fit using f_{drying} approach and this was consistent with the results by [18] in which the approach outperformed the other two approaches. The three approaches underestimated ET and this

may be suggestive of overestimation of the measured latent and sensible heat fluxes since our accompanying paper showed evidence of possible advection[29]. Consequently, this over-estimation of the vertical heat fluxes results in the apparent underestimation by the model. Furthermore, this could also be explained by complex behaviour of the vegetation with respect to its high water storage potential and phenological control of stomata to optimize [29] water use. With respect to the RMSE for the three approaches, most of the error was unsystematic, suggesting that all the three approaches were valuable in modelling ET.

The results of model sensitivity analysis suggest that the PML model was highly sensitive to the LAI and aerodynamic components. Therefore, it is crucial to accurately determine these if the PML is to be accurately implemented. Although albedo was an important input, the model was less sensitive to dynamics in albedo. Our results also suggest that the convergent evolution of the AT vegetation results in further uncertainties in the model since the biophysical model may fail to reproduce vegetation control to ET. In addition, the model may not be able to capture dynamics in the plant available water owing to the very high water storage capacity of the vegetation and the possibility of plants capturing groundwater. This may mean that the observed ET may not necessarily be connected to SWC measured at a depth of 25 mm. Other uncertainties in the model are related to upstream data related to the MODIS products used in the models. However, MODIS data have been widely used and yielded good results comparable to measurements.

4. CONCLUSION

We evaluated the applicability of the PML in a dryland of South Africa dominated by thicket vegetation. We found that convergent evolution of vegetation presented unique challenges to ET modelling. The phenological characteristics related to stomata control, the high water storage capacity of the vegetation and possibilities of them accessing ground water makes ET modelling a daunting task in the study area. In addition, the relationship between measured SWC and ET was complex as the two did not always show strong connection. Despite these challenges reasonable model fit was observed. Quantifying available plant water in such landscapes remains a challenge and improvement in this direction may improve the model fit.

ACKNOWLEGDEMENTS

The research was supported by the National Research Foundation of South Africa (National Equipment Programme) and the Water Research Commission (project K5/2400/4)

REFERENCES

[1] McMahon, T. A., Peel, M. C., Lowe, L., Srikanthan, R., McVicar, T. R., “Estimating actual, potential, reference crop and pan evaporation using standard meteorological data: a pragmatic synthesis,” Hydrol. Earth Syst. Sci. **17**(4), 1331–1363 (2013).

[2] Liou, Y.-A., Kar, S., “Evapotranspiration Estimation with Remote Sensing and Various Surface Energy Balance Algorithms—A Review,” Energies **7**(5), 2821–2849 (2014).

[3] Liu, J.., Yang, H., “Spatially explicit assessment of global consumptive water uses in cropland: Green and blue water,” J. Hydrol. **384**(3-4), 187–197, Elsevier B.V. (2010).

[4] Hoff, H., Falkenmark, M., Gerten, D., Gordon, L., Karlberg, L.., Rockström, J., “Greening the global water system,” J. Hydrol. **384**(3-4), 177–186, Elsevier B.V. (2010).

[5] Barbour, M. M., Hunt, J. E., Walcroft, A. S., Rogers, G. N. D., McSeveny, T. M.., Whitehead, D., “Components of ecosystem evaporation in a temperate coniferous rainforest, with canopy transpiration scaled using sapwood density,” New Phytol. **165**(2), 549–558 (2005).

[6] Foken, T., Aubinet M. and Leuning, R., “ The Eddy Covariance Method,” In Aubinet, M., Vesala T. and Papale D. (eds.) [Eddy covariance: A practical guide to measurement and data analysis], Springer Science+Business Media B.V. 2012, Springer Dordrecht, Heidelberg London, New York.pp 1-22 (2012).

[7] Amatya, D. M., Irmak, S., Gowda, P., Sun, G., Nettles, J. E.., Douglas-Mankin, K. R., "Ecosystem Evapotranspiration: Challenges in Measurements, Estimates, and Modeling," Trans. ASABE **59**(2), 555–560 (2016).
[8] Li, Z.-L., Tang, R., Wan, Z., Bi, Y., Zhou, C., Tang, B., Yan, G.., Zhang, X., "A review of current methodologies for regional evapotranspiration estimation from remotely sensed data.," Sensors (Basel). **9**(5), 3801–3853 (2009).
[9] García, M., Sandholt, I., Ceccato, P., Ridler, M., Mougin, E., Kergoat, L., Morillas, L., Timouk, F., Fensholt, R., Domingo, F., "Actual evapotranspiration in drylands derived from in-situ and satellite data: Assessing biophysical constraints," Remote Sens. Environ. **131**, 103–118 (2013).
[10] Fisher, J. B., Tu, K. P.., Baldocchi, D. D., "Global estimates of the land-atmosphere water flux based on monthly AVHRR and ISLSCP-II data, validated at 16 FLUXNET sites," Remote Sens. Environ. **112**(3), 901–919 (2008).
[11] Moran, M. S., Rahman, a. F., Washburne, J. C., Goodrich, D. C., Weltz, M. a.., Kustas, W. P., "Combining the Penman-Monteith equation with measurements of surface temperature and reflectance to estimate evaporation rates of semiarid grassland," Agric. For. Meteorol. **80**(2-4), 87–109 (1996).
[12] Cleugh, H. A., Leuning, R., Mu, Q., Running, S. W., "Regional evaporation estimates from flux tower and MODIS satellite data," Remote Sens. Environ. **106**(3), 285–304 (2007).
[13] Zhang, Y. Q., Chiew, F. H. S., Zhang, L., Leuning, R., Cleugh, H. A., "Estimating catchment evaporation and runoff using MODIS leaf area index and the Penman-Monteith equation," Water Resour. Res. **44**(10), n/a – n/a (2008).
[14] Monteith, J. L., "Evaporation and environment.," Symp. Soc. Exp. Biol. **19**, 205–234 (1965).
[15] Villagarcía, L., Were, a., Domingo, F., García, M., Alados-Arboledas, L., "Estimation of soil boundary-layer resistance in sparse semiarid stands for evapotranspiration modelling," J. Hydrol. **342**(1-2), 173–183 (2007).
[16] Leuning, R. Zhang Y. Q., Rajaud, A. Cleugh. H., Tu. K., "A simple surface conductance model to estimate regional evaporation using MODIS leaf area index and the Penman-Monteith equation," Water Resour. Res. (2008).
[17] Morillas, L., Leuning, R., Villagarc, L., García, M., Serrano-Ortiz, P., Domingo, F., "Improving evapotranspiration estimates in Mediterranean drylands : The role of soil evaporation," 6572–6586 (2013).
[18] Ventura, F., Snyder, R. L.., Bali, K. M., "Estimating Evaporation from Bare Soil Using Soil Moisture Data," J. Irrig. Drain. Eng. **132**(April), 153–158 (2006).
[19] Zhang, Y., Leuning, R., Hutley, L. B., Beringer, J., Mchugh, I.., Walker, J. P., "Using long - term water balances to parameterize surface conductances and calculate evaporation at 0 . 05 ° spatial resolution," Water Resour. Res. **46**, 1–14 (2010).
[20] Priestley, C. H. B.., Taylor, R. J., "On the assessment of surface heat flux and evaporation using large-scale parameters," Mon. Weather Rev. **100**(February), 81–82 (1972).
[21] Mu, Qiaozhen, Faith Ann Heinsch, Z. M.., Running, S. W., "Regional evaporation estimates from flux tower and MODIS satellite data," Remote Sens. Environ. **106**(3), 285–304 (2007).
[22] Cleugh, H. A., Leuning, R., Mu, Q., Running, S. W., "Regional evaporation estimates from flux tower and MODIS satellite data," Remote Sens. Environ. **106**(3), 285–304 (2007).
[23] Borland, A. M., Griffiths, H., Hartwell, J.., Smith, J. A. C., "Exploiting the potential of plants with crassulacean acid metabolism for bioenergy production on marginal lands," J. Exp. Bot. **60**(10), 2879–2896 (2009).
[24] Carr, M. K. V., "The Water Relations and Irrigation Requirements of Passion Fruit (Passiflora Edulis Sims): a Review," Exp. Agric. **49**(4), 585–596 (2013).
[25] Owen, N. A., Choncubhair, Ó. N., Males, J., del Real Laborde, J. I., Rubio-Cortés, R., Griffiths, H.., Lanigan, G., "Eddy covariance captures four-phase crassulacean acid metabolism (CAM) gas exchange signature in Agave," Plant, Cell Environ. **39**(2), 295–309 (2016).
[26] "Hoare, D.B., Mucina, L., Rutherford, M.C., Vlok, J.H.J., Euston-Brown, D.I.W., Palmer, A.P., Powreie, L.W., Lechmere-Oerttel, R.G., Proches, S.M., Dold, A.P. and Wart, R.A., "Albany Thicket Biome," In Mucina L, Rutherford MC, (eds.), [The vegetation of South Africa, Lesotho and Swaziland]. *Strelitzia* 19, South African National Boidiversity Institute, Pretoria, 540-567(2006).
[27] Mills, A. J., Cowling, R. M., "Rate of carbon sequestration at two thicket restoration sites in the Eastern Cape, South Africa," Restor. Ecol. **14**(1), 38–49 (2006).
[28] Schulze, R.E., [South African Atlas of Agrohydrology and Climatology], WRC Report TT82/96, Water Research

Commission, Pretoria (1997).
[29] Gwate O., Mantel, S.K., Palmer, AR., Gibson, L.A. "Measuring evapotranspiration using an eddy covariance system over a subtropical thicket of the Eastern Cape, South Africa , SPIE Remote sensing 2016."
[30] Campbell Scientific., Model HFP01 Soil Heat Flux Plate, Instruction Manual (2002).
[31] Myneni, R., Knyazikhin, Y., Glassy, J., Votava, P.., Shabanov, N., "User' s Guide FPAR, LAI (ESDT: MOD15A2) 8-day Composite NASA MODIS Land Algorithm," Terra, 1–17 (2003).
[32] Liang, S., "Narrowband to broadband conversions of land surface albedo I Algorithms," Remote Sens. Environ. **76**(2000), 213–238 (2001).
[33] Vickers, D.., Mahrt, L., "Quality control and flux sampling problems for tower and aircraft data," J. Atmos. Ocean. Technol. **14**(3), 512–526 (1997).
[34] Finkelstein, L.P., & S. P. ., "Sampling error in eddy correlation flux measurements," Geophys. Res. **106**(D4), 3503–3509 (2001).
[35] Mauder, M.., Foken, T., "Quality control of eddy covariance measurements (C: 0,1,2)," 29–31 (2004).
[36] Falge, E., Baldocchi, D.., Olson, R., "Gap filling strategies for long term energy flux data sets," Agric. For. Meteorol.(107), 71–77 (2001).
[37] Kljun, N., Calanca, P., Rotach, M. W.., Schmid, H. P., "A simple parameterisation for flux footprint predictions," Boundary-Layer Meteorol. **112**(3), 503–523 (2004).
[38] "CLIMWAT 2.0 for CROPWAT (FAO water (2013), 14 June 2015, http://www.fao.org/nr/water/infores_databases_climwat.html
[39] Mebane, W. R. J.., Sekhon, J. S., "Genetic Optimization Using Derivatives: The The rgenoud Package for R," J. Stat. Softw. **42**(11), 1 – 26 (2011).
[40] Mebane, A. W. R., "Package ' rgenoud '" (2015), 4 August 2016, https://cran.r-project.org/web/packages/rgenoud/rgenoud.pdf
[41] Legendre, P., "Model II regression user's guide, R edition," R Vignette **4**, 1–14 (2013), 27 July 2016, https://cran.r-project.org/web/packages/lmodel2/vignettes/mod2user.pdf.
[42] Willmott, C. J., "Some comments on the evaluation of model performance," Bulltin Am. Meteorol. Soc., 1309–1313 (1982).
[43] Willmott, J. C., "On the validation of models," Phys. Geogr. **2**(2), 184–194 (1981).
[44] Moriasi, D. N., Arnold, J. G., Van Liew, M. W., Binger, R. L., Harmel, R. D.., Veith, T. L., "Model evaluation guidelines for systematic quantification of accuracy in watershed simulations," Trans. ASABE **50**(3), 885–900 (2007).
[45] A. Al-Busaidi, T., Yamamoto, T., Tanak, S., Moritani, S., "Evapotranspiration of Succulent Plant (Sedum)" (2013), 17 April 2016, http://cdn.intechopen.com/pdfs-wm/40958.pdf
[46] Mu, Q., Zhao, M.., Running, S. W., "Improvements to a MODIS global terrestrial evapotranspiration algorithm," Remote Sens. Environ. **115**(8), 1781–1800, Elsevier Inc. (2011).
[47] Kelliher, F. M., Leuning, R., Raupach, M. R., Schulze, E. D., "Maximum conductances for evaporation from global vegetation types," Agric. For. Meteorol. **73**(1-2), 1–16 (1995).